Achievability of Fluid Antenna Multiple Access: A Han-Kobayashi's Comparison

Wee Kiat New[§], Kai-Kit Wong[§,‡], Hao Xu[§], Kin-Fai Tong[§] and Chan-Byoung Chae[‡]
[§]Department of Electronic and Electrical Engineering, University College London, London, United Kingdom
[‡]School of Integrated Technology, Yonsei University, Seoul, Korea
Email: {a.new, kai-kit.wong, hao.xu, k.tong}@ucl.ac.uk, cbchae@yonsei.ac.kr

***Abstract*—Recently, fluid antenna system (FAS) has emerged as a potential candidate to deliver extra diversity and multiplexing gains. This new technology can also be adopted to mitigate interference namely, fluid antenna multiple access (FAMA). Unlike existing schemes, the key concept of FAMA is to communicate at a spatial moment where the interference is in deep fade. However, FAMA treats interference as noise and it remains unclear whether such a strategy is capacity-efficient. To address this question, we leverage insights from information theory and introduce a new Han-Kobayashi (HK)-FAMA scheme that considers rate splitting, power splitting and joint decoding, to be a capacity benchmark. Using this capacity benchmark, we then illustrate that FAMA (alone without HK) can be near to being optimal despite its simplicity. Besides, we employ a new performance metric based on the generalized degree-of-freedom (gdof) to explain the principle of FAMA.**

***Index Terms*—6G, fluid antenna system, fluid antenna multiple access, Han-Kobayashi scheme.**

I. Introduction

Driven by various emerging use cases and applications, the sixth-generation (6G) networks are expected to support numerous requirements. Some of these expectations may include a peak rate of 1 Tbps, a minimum latency of 0.1 ms, a reliability of 99.9999% and massive connectivity of 10^7 devices/km^2. To meet these demands, it is necessary to explore new technology that can make a performance leap. In this regard, fluid antenna system (FAS) has emerged as a potential candidate for 6G to deliver extra diversity and multiplexing gains [1].

FAS represents *any* software-controllable fluidic, conductive, dielectric structure or radio-frequency (RF) pixels that can change its shape and position to reconfigure the radiation characteristics. The simplest setup consists of one RF-chain and M preset locations (known as ports) that are distributed in a given space. The radiating element can switch to the best port to obtain the most desirable channel. Several prototypes have also been developed in recent years [1], [2]. Motivated by its flexibility and practicality, recent studies in [2]–[5] have shown that FAS greatly improves the communication rate and reliability over the traditional antenna system (TAS), in which the antenna is fixed in position (e.g., $M = 1$).

With the unique ability to switch the antenna position finely in space, FAS can also be used to mitigate interference.[1] This stems from the idea that a receiver can find an opportunity in the spatial domain to receive information while the interference suffers from a deep fade. This scheme is referred to as fluid antenna multiple access (FAMA) [6]. Compared to existing techniques, FAMA offers a new possibility where precoding at the transmitter and successive interference cancellation at the receiver are not necessary. Moreover, FAMA can be classified into fast FAMA and slow FAMA. In fast FAMA, the receiver switches its port on a per-symbol basis while in slow FAMA, the receiver switches its port when the channel changes. This paper focuses on the latter. It is shown in [6] that slow FAMA can serve up to a few receivers on the same radio resource (e.g., frequency/time) while the interference can be aggregated as one [1]. The analytical outage probability of two-user slow FAMA was recently derived in [7].

Despite its potential, FAMA simply treats interference as noise and it remains unclear whether this strategy is capacity-efficient. To address this, we leverage insights from information theory and observe that for a specific port, the multiple-input single-output (MISO) broadcast channel in [7] can be viewed as an interference channel (IC) since precoding is not employed. In fact, rate splitting multiple access is inspired by the reverse approach, i.e., viewing the IC as a MISO broadcast channel [8]. To the best of our knowledge, the capacity of IC is still unknown, even in the Gaussian case. Nevertheless, it is widely known that the best achievable scheme in a two-user Gaussian IC is the Han-Kobayashi (HK) scheme [9], [10]. Specifically, [9] showed that a simple HK scheme (without time sharing or optimal power splitting) is capable of achieving the capacity to within one bit. Nevertheless, the performance of the HK scheme is extremely complicated since it includes all the known strategies as its special cases [10]. Fortunately, through decades of efforts [9]–[13], the performance of the HK scheme in different regimes is now more understood.

The goal of this paper is to understand the effectiveness of FAMA in terms of achieving the capacity. Motivated by the above-mentioned developments, we consider two transmitter-receiver pairs in which each receiver is equipped with a 2D surface fluid antenna. In this setting, we first introduce a new HK-FAMA scheme that further considers rate splitting, power splitting and joint decoding while also having the ability of FAS to reconfigure the channel. We then maximize the sum-rate of the HK-FAMA technique by jointly optimizing port selection, power splitting and rate splitting. Our results show

[1]Note that FAS can have few hundred or more ports within an area of λ^2. This offers a new method to mitigate interference which cannot be achieved using antenna selection as it is impractical to have few hundreds of physical antennas within the same amount of area.

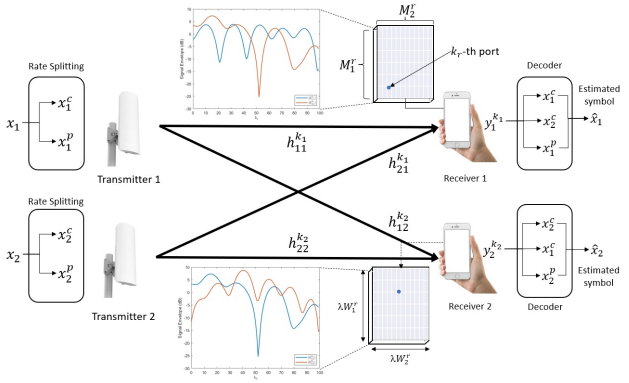

Figure 1. A schematic of HK-FAMA with two transmitter-receiver pairs.

that FAMA can be near to being optimal. Furthermore, we use a new performance metric to reveal the principle of FAMA.

II. System Model

As shown in Fig. 1, we consider two pairs of transmitter and receiver. Each transmitter sends information to its respective receiver but it interferes with the other receiver. Each transmitter is equipped with a traditional antenna while each receiver is equipped with a 2D surface fluid antenna which consists of M_r preset locations (known as ports) that are uniformly distributed in an area of W_r where $r \in \{1,2\}$. Specifically, we consider a grid structure where M_i^r ports are uniformly distributed along a linear space of length λW_i^r, where $i \in \{1,2\}$ and λ is the wavelength of the carrier frequency. Thus, we have $M_r = M_1^r \times M_2^r$ and $W_r = W_1^r \times W_2^r$. Unlike a traditional antenna, the radiating element can switch its location among these M_r ports to flexibly adjust the received signal strength. If the radiating element is always fixed at a specific port, it is then equivalent to a traditional antenna.

We refer to each port as the (m_1^r, m_2^r)-th port. Furthermore, we introduce an arbitrary one-to-one function so that $f\left(m_1^r, m_2^r\right) = k_r$ and $f^{-1}\left(k_r\right) = \left(m_1^r, m_2^r\right)$ where $k_r \in \{1,\ldots,M_r\}$, for $m_1^r \in \{1,\ldots,M_1^r\}$ and $m_2^r \in \{1,\ldots,M_2^r\}$. In a 3D environment with rich scattering, the spatial correlation between the k_r-th port and ℓ_r-th port is given by [5]

$$J_{k_r,\ell_r}^r = j_0\left(2\pi\sqrt{\left(\frac{\left|m_1^r-\tilde{m}_1^r\right|}{M_1^r-1}W_1^r\right)^2+\left(\frac{\left|m_2^r-\tilde{m}_2^r\right|}{M_2^r-1}W_2^r\right)^2}\right), \tag{1}$$

where $j_0\left(\cdot\right)$ denotes the spherical Bessel function of the first kind, $f\left(\tilde{m}_1^r, \tilde{m}_2^r\right) = \ell_r$ and $f^{-1}\left(\ell_r\right) = \left(\tilde{m}_1^r, \tilde{m}_2^r\right)$ with $\ell_r \in \{1,\ldots,M_r\}$, $\tilde{m}_1^r \in \{1,\ldots,M_1^r\}$ and $\tilde{m}_2^r \in \{1,\ldots,M_2^r\}$. The spatial correlation matrix $\boldsymbol{J}_r$ is expressed as

$$\boldsymbol{J}_r = \begin{bmatrix} J_{1,1}^r & J_{1,2}^r & \cdots & J_{1,M_r}^r \\ J_{2,1}^r & J_{2,2}^r & \cdots & \vdots \\ \vdots & \vdots & \ddots & \vdots \\ J_{M_r,1}^r & J_{M_r,2}^r & \cdots & J_{M_r,M_r}^r \end{bmatrix}. \tag{2}$$

Using eigenvalue decomposition, $\boldsymbol{J}_r$ can be decomposed into $\boldsymbol{J}_r = \boldsymbol{U}_r\boldsymbol{\Lambda}_r\boldsymbol{U}_r^H$ where $\boldsymbol{U}_r = \left[\boldsymbol{u}_1^r, \boldsymbol{u}_2^r, \ldots, \boldsymbol{u}_{M_r}^r\right]$ and $\boldsymbol{\Lambda}_r = \mathrm{diag}\left(\lambda_1^r, \lambda_2^r, \ldots, \lambda_{M_r}^r\right)$. More concisely, the column vector $\boldsymbol{u}_l^r$ is the l-th eigenvector of $\boldsymbol{J}_r$ and λ_l^r is the corresponding eigenvalue of $\boldsymbol{u}_l^r$. According to [4], the complex channel from transmitter t to receiver r can be modelled as

$$\boldsymbol{h}_{tr} = \sigma_{tr}\boldsymbol{U}_r\sqrt{\boldsymbol{\Lambda}_r}\boldsymbol{g} = \begin{bmatrix} h_{tr}^1 & h_{tr}^2 & \cdots & h_{tr}^{M_r} \end{bmatrix}^T, \tag{3}$$

where $t \in \{1,2\}$, σ_{tr}^2 denotes the large-scale fading between transmitter t and receiver r, $\boldsymbol{g}$ denotes a circularly symmetric complex Gaussian vector with independent and identically distributed (i.i.d.) entries such that each entry has a zero mean and unit variance and $(\cdot)^T$ is the transpose operator. For ease of expositions, we denote t' and r' as the complement of t and r, respectively. If $r = 1$, then $r' = 2$ and vice versa.

Furthermore, we introduce a new HK-FAMA scheme which is useful for evaluating the performance of different schemes. In HK-FAMA, the receiver's information signal is split into two parts: public message and private message. For public messages, a common codebook is employed while for private messages different codebooks are employed. The information signal of receiver r can be expressed as [8]

$$x_r = \sqrt{1-\gamma_t}x_r^c + \sqrt{\gamma_t}x_r^p, \tag{4}$$

where x_r^c is the public message of receiver r and x_r^p is the private message of receiver r such that $\mathbb{E}[|x_r^c|^2] = \mathbb{E}[|x_r^p|^2] = 1$. Furthermore, we have $\gamma_t \in [0,1], \forall t$. Note that the public messages can be decoded by both of the receivers (i.e., r and r') while the private message can only be decoded by the intended receiver (i.e., r). Without loss of generality, we assume that the average transmit power at transmitter t is P_t, and $\bar{\gamma}_t = (1-\gamma_t)$ and γ_t are the fraction of powers allocated to the public and private messages, respectively.

Unlike traditional antenna, the radiating element of the receiver r can switch its location among the M_r ports. Thus, the received signal of receiver r at the k_r-th port is expressed as

$$y_r^{k_r} = h_{tr}^{k_r}x_r + h_{t'r}^{k_r}x_{r'} + z_r^{k_r}, \tag{5}$$

where $z_r^{k_r}$ is the additive white Gaussian noise of receiver r at the k_r-th port with zero mean and variance of N_r. Suppose that the radiating element of the receiver r is switched to the k_r-th port and the power allocated to the private message of receiver r is $\gamma_r P_r, \forall r$ (i.e., $t = r$), then the rates of the public message and private message of receiver r are R_r^c and R_r^p, respectively. Hence, the achievable rate of receiver r is given by

$$R_r^{\mathrm{HKF}} = R_r^c + R_r^p. \tag{6}$$

For brevity, no time sharing is considered in this paper. For a fixed $\boldsymbol{k} = [k_1, k_2]^T$ and $\boldsymbol{\gamma} = [\gamma_1, \gamma_2]^T$, the rate pairs of HK-FAMA must satisfy the following constraints [13]:

$$R_1^{\mathrm{HKF}} \le \log\left(1+\frac{\left|h_{11}^{k_1}\right|^2 P_1}{\gamma_2\left|h_{21}^{k_1}\right|^2 P_2+N_1}\right), \tag{7a}$$

$$R_2^{\mathrm{HKF}} \le \log\left(1+\frac{\left|h_{22}^{k_2}\right|^2 P_2}{\gamma_1\left|h_{12}^{k_2}\right|^2 P_1+N_2}\right), \tag{7b}$$

$$R_1^{\mathrm{HKF}} + R_2^{\mathrm{HKF}} \le \log\left(1 + \frac{\left|h_{11}^{k_1}\right|^2 P_1 + \bar{\gamma}_2 \left|h_{21}^{k_1}\right|^2 P_2}{\gamma_2 \left|h_{21}^{k_1}\right|^2 P_2 + N_1}\right) + \log\left(1 + \frac{\gamma_2 \left|h_{22}^{k_2}\right|^2 P_2}{\gamma_1 \left|h_{12}^{k_2}\right|^2 P_1 + N_2}\right), \tag{7c}$$

$$R_1^{\mathrm{HKF}} + R_2^{\mathrm{HKF}} \le \log\left(1 + \frac{\left|h_{22}^{k_2}\right|^2 P_2 + \bar{\gamma}_1 \left|h_{12}^{k_2}\right|^2 P_1}{\gamma_1 \left|h_{12}^{k_2}\right|^2 P_1 + N_2}\right) + \log\left(1 + \frac{\gamma_1 \left|h_{11}^{k_1}\right|^2 P_1}{\gamma_2 \left|h_{21}^{k_1}\right|^2 P_2 + N_1}\right), \tag{7d}$$

$$R_1^{\mathrm{HKF}} + R_2^{\mathrm{HKF}} \le \log\left(1 + \frac{\gamma_1 \left|h_{11}^{k_1}\right|^2 P_1 + \bar{\gamma}_2 \left|h_{21}^{k_1}\right|^2 P_2}{\lambda_2 \left|h_{21}^{k_1}\right|^2 P_2 + N_1}\right) + \log\left(1 + \frac{\gamma_2 \left|h_{22}^{k_2}\right|^2 P_2 + \bar{\gamma}_1 \left|h_{12}^{k_2}\right|^2 P_1}{\lambda_1 \left|h_{12}^{k_2}\right|^2 P_1 + N_2}\right), \tag{7e}$$

$$2R_1^{\mathrm{HKF}} + R_2^{\mathrm{HKF}} \le \log\left(1 + \frac{\left|h_{11}^{k_1}\right|^2 P_1 + \bar{\gamma}_2 \left|h_{21}^{k_1}\right|^2 P_2}{\gamma_2 \left|h_{21}^{k_1}\right|^2 P_2 + N_1}\right) + \log\left(1 + \frac{\gamma_1 \left|h_{11}^{k_1}\right|^2 P_1}{\gamma_2 \left|h_{21}^{k_1}\right|^2 P_2 + N_1}\right) + \log\left(1 + \frac{\gamma_2 \left|h_{22}^{k_2}\right|^2 P_2 + \bar{\gamma}_1 \left|h_{12}^{k_2}\right|^2 P_1}{\gamma_1 \left|h_{12}^{k_2}\right|^2 P_1 + N_2}\right), \tag{7f}$$

$$R_1^{\mathrm{HKF}} + 2R_2^{\mathrm{HKF}} \le \log\left(1 + \frac{\gamma_1 \left|h_{11}^{k_1}\right|^2 P_1 + \bar{\gamma}_2 \left|h_{21}^{k_1}\right|^2 P_2}{\lambda_2 \left|h_{21}^{k_1}\right|^2 P_2 + N_1}\right) + \log\left(1 + \frac{\left|h_{22}^{k_2}\right|^2 P_2 + \bar{\gamma}_1 \left|h_{12}^{k_2}\right|^2 P_1}{\gamma_1 \left|h_{12}^{k_2}\right|^2 P_1 + N_2}\right) + \log\left(1 + \frac{\gamma_2 \left|h_{22}^{k_2}\right|^2 P_2}{\gamma_1 \left|h_{12}^{k_2}\right|^2 P_1 + N_2}\right). \tag{7g}$$

If $k_r, \forall r$ is fixed, then the HK-FAMA scheme is equivalent to the traditional HK scheme.

III. Maximum Sum-Rate of HK-FAMA

We aim to maximize the sum-rate of HK-FAMA via joint optimization of port selection, power splitting and rate splitting. The optimization problem is formulated as

$$\max_{\boldsymbol{k}\in\mathcal{K},\boldsymbol{\lambda}\in\Gamma \atop \boldsymbol{R}_{\mathrm{HKF}}\in\mathcal{R}} R_1^{\mathrm{HKF}} + R_2^{\mathrm{HKF}}, \tag{8}$$

where $\mathcal{K} = \{[k_1, k_2]^T | k_r \in \{1, \ldots, M_r\}, \forall r\}$, $\Gamma = \{[\gamma_1, \gamma_2]^T | \gamma_1, \gamma_2 \in [0, 1]\}$ and $\mathcal{R}$ is the set of achievable rate pairs $\boldsymbol{R}_{\mathrm{HKF}} = \left[R_1^{\mathrm{HKF}}, R_2^{\mathrm{HKF}}\right]^T$ that satisfies (7). Since the constraints in (7) are non-convex with respect to $\boldsymbol{\gamma}$ and $\mathcal{K}$ is a non-convex set, (8) is a non-convex optimization problem.

To solve this globally, we divide the optimization problem into three hierarchical subproblems: optimal port problem, optimal power splitting problem and optimal rate splitting problem. Specifically, given a fixed $\boldsymbol{k}$ and $\boldsymbol{\gamma}$, the sum-rate of HK-FAMA can be maximized via the following optimization problem:

$$\max_{\boldsymbol{R}_{\mathrm{HKF}}\in\mathcal{R}} R_1^{\mathrm{HKF}} + R_2^{\mathrm{HKF}}. \tag{9}$$

Interestingly, (9) is a linear optimization problem because the right hand sides of (7) are constants if $\boldsymbol{k}$ and $\boldsymbol{\gamma}$ are given and thus the solution can be easily obtained. Let us denote the global optimal value of (9) as $R^*_{\mathrm{HKF}}(\boldsymbol{k}, \boldsymbol{\gamma})$. Given a fixed $\boldsymbol{k}$, we can obtain the optimal power splitting by solving

$$\max_{\boldsymbol{\gamma}\in\Gamma} R^*_{\mathrm{HKF}}(\boldsymbol{k}, \boldsymbol{\gamma}), \tag{10}$$

which is a very challenging optimization problem. Nevertheless, the global optimal value to this optimization problem, which is denoted as $R^*_{\mathrm{HKF}}(\boldsymbol{k})$, can be found in very complicated expressions through a collection of works [10]–[12].

By analyzing their expressions, we further classify the interference level into 16 regimes in order to obtain the optimal value and the optimal power splitting of (10) in a single closed-form expression.[2] The complete solutions are summarized in Table I where we have defined as

$$C_0 = \log\left(1 + \frac{P_1\left|h_{11}^{k_1}\right|^2}{N_1}\right) + \log\left(1 + \frac{P_2\left|h_{22}^{k_2}\right|^2}{N_2}\right),$$

$$C_1 = \log\left(1 + \frac{P_2\left|h_{22}^{k_2}\right|^2}{P_1|h_{12}|^2 + N_2}\right) + \log\left(1 + \frac{P_1\left|h_{12}^{k_2}\right|^2}{N_2}\right),$$

$$C_2 = \log\left(1 + \frac{P_1\left|h_{11}^{k_1}\right|^2}{P_2\left|h_{21}^{k_1}\right|^2 + N_1}\right) + \log\left(1 + \frac{P_2\left|h_{21}^{k_1}\right|^2}{N_1}\right),$$

$$C_3 = \log\left(1 + \frac{P_2\left|h_{22}^{k_2}\right|^2}{P_1\left|h_{12}^{k_2}\right|^2 + N_2}\right) + \log\left(1 + \frac{P_1\left|h_{11}^{k_1}\right|^2}{N_1}\right),$$

$$C_4 = \log\left(1 + \frac{P_1\left|h_{11}^{k_1}\right|^2}{P_2\left|h_{21}^{k_1}\right|^2 + N_1}\right) + \log\left(1 + \frac{P_2\left|h_{22}^{k_2}\right|^2}{N_2}\right),$$

$C_5 = C_2 + g\left(\tilde{\lambda}_1, \tilde{\lambda}_2\right)$, $C_6 = C_2 + g\left(\hat{\lambda}_1\hat{\lambda}_2\right)$ and

$$C_7 = \log\left(1 + \frac{P_1\left|h_{11}^{k_1}\right|^2}{P_2\left|h_{21}^{k_1}\right|^2 + N_1}\right) + \log\left(1 + \frac{P_2\left|h_{22}^{k_2}\right|^2}{P_1\left|h_{12}^{k_2}\right|^2 + N_2}\right).$$

Furthermore, we denote

$$g(\lambda_1, \lambda_2) = \log\left(1 + \frac{\lambda_2 P_2\left|h_{22}^{k_2}\right|^2}{\lambda_1 P_1\left|h_{12}^{k_2}\right|^2 + N_2}\right) - \log\left(1 + \frac{\lambda_2 P_2\left|h_{21}^{k_1}\right|^2}{N_1}\right),$$

$$f(\lambda_1, \lambda_2) = \frac{N_1\left(N_2 + \lambda_2 P_2\left|h_{22}^{k_2}\right|^2 + \lambda_1 P_1\left|h_{12}^{k_2}\right|^2\right)}{\left(N_1 + \lambda_2 P_2\left|h_{21}^{k_1}\right|^2\right)\left(N_2 + \lambda_1 P_1\left|h_{12}^{k_2}\right|^2\right)}, \; n \ge 0, \; \hat{\lambda}_1 = m\hat{\lambda}_2 + n, \; \hat{\lambda}_2 = \left[\frac{-q_1 \pm \sqrt{q_1^2 - 4q_2}}{2}\right]_0^+, \; q_1 = \frac{2\left(P_1\left|h_{12}^{k_2}\right|^2 n + N_2\right)}{P_1\left|h_{12}^{k_2}\right|^2 m + P_2\left|h_{22}^{k_2}\right|^2}$$

and $q_2 = \frac{N_2 + P_1\left|h_{12}^{k_2}\right|^2 n}{P_1\left|h_{12}^{k_2}\right|^2\left|h_{21}^{k_1}\right|^2 m} \frac{\left(|h_{21}|^2\left(P_1\left|h_{12}^{k_2}\right|^2 n + N_2\right) - \left|h_{22}^{k_2}\right|^2 N_1\right)}{\left(P_1\left|h_{12}^{k_2}\right|^2 m + P_2\left|h_{22}^{k_2}\right|^2\right)}$

where

$$c = \frac{N_1\left(N_2 + P_2\left|h_{22}^{k_2}\right|^2 + P_1\left|h_{12}^{k_2}\right|^2\right)}{N_2\left(N_1 + P_1\left|h_{11}^{k_1}\right|^2 + P_2\left|h_{21}^{k_1}\right|^2\right)}$$

$$m = \frac{P_2\left(\left|h_{22}^{k_2}\right|^2 N_1 - \left|h_{21}^{k_1}\right|^2 N_2 + P_1\left(\left|h_{22}^{k_2}\right|^2\left|h_{11}^{k_1}\right|^2 - \left|h_{21}^{k_1}\right|^2\left|h_{12}^{k_2}\right|^2\right)\right)}{P_1\left(\left|h_{11}^{k_1}\right|^2 N_2 - \left|h_{12}^{k_2}\right|^2 N_1 + P_2\left(\left|h_{22}^{k_2}\right|^2\left|h_{11}^{k_1}\right|^2 - \left|h_{21}^{k_1}\right|^2\left|h_{12}^{k_2}\right|^2\right)\right)},$$

[2]Different from [10], we derive the complete solutions here which include strong and mixed interference levels. Moreover, this paper presents new conditions for weak interference level as the ones in [10] are inaccurate.

Table I
SUMMARY OF THE SOLUTIONS TO (10)

Interference level	Conditions	$R^*_{\mathrm{HKF}}(\boldsymbol{k})$	(γ_1^*, γ_2^*)
Very strong	$\frac{\left\|h_{21}^{k_1}\right\|^2}{\left\|h_{22}^{k_2}\right\|^2} \geq \frac{N_1}{N_2} + \frac{P_1\left\|h_{11}^{k_1}\right\|^2}{N_2}, \frac{\left\|h_{12}^{k_2}\right\|^2}{\left\|h_{11}^{k_1}\right\|^2} \geq \frac{N_2}{N_1} + \frac{P_2\left\|h_{22}^{k_2}\right\|^2}{N_1}$,	C_0	$(0,0)$
Mixedly strong I	$\frac{\left\|h_{21}^{k_1}\right\|^2}{\left\|h_{22}^{k_2}\right\|^2} \geq \frac{N_1}{N_2} + \frac{P_1\left\|h_{11}^{k_1}\right\|^2}{N_2}, \frac{N_2}{N_1} + \frac{P_2\left\|h_{22}^{k_2}\right\|^2}{N_1} \geq \frac{\left\|h_{12}^{k_2}\right\|^2}{\left\|h_{11}^{k_1}\right\|^2} \geq \frac{N_2}{N_1}$	C_1	$(0,0)$
Mixedly strong II	$\frac{N_1}{N_2} + \frac{P_1\left\|h_{11}^{k_1}\right\|^2}{N_2} \geq \frac{\left\|h_{21}^{k_1}\right\|^2}{\left\|h_{22}^{k_2}\right\|^2} \geq \frac{N_2}{N_1}, \frac{\left\|h_{12}^{k_2}\right\|^2}{\left\|h_{11}^{k_1}\right\|^2} \geq \frac{N_2}{N_1} + \frac{P_2\left\|h_{22}^{k_2}\right\|^2}{N_1}$	C_2	$(0,0)$
Newly strong I	$\frac{N_1}{N_2} + \frac{P_1\left\|h_{11}^{k_1}\right\|^2}{N_2} \geq \frac{\left\|h_{21}^{k_1}\right\|^2}{\left\|h_{22}^{k_2}\right\|^2} \geq \frac{N_1}{N_2}, \frac{N_2}{N_1} + \frac{P_2\left\|h_{22}^{k_2}\right\|^2}{N_1} \geq \frac{\left\|h_{12}^{k_2}\right\|^2}{\left\|h_{11}^{k_1}\right\|^2} \geq \frac{N_2}{N_1}, \frac{P_1\left(\left\|h_{11}^{k_1}\right\|^2 N_2 - \left\|h_{12}^{k_2}\right\|^2 N_1\right)}{P_2\left(\left\|h_{22}^{k_2}\right\|^2 N_1 - \left\|h_{21}^{k_1}\right\|^2 N_2\right)} \geq 1$	C_1	$(0,0)$
Newly strong II	$\frac{N_1}{N_2} + \frac{P_1\left\|h_{11}^{k_1}\right\|^2}{N_2} \geq \frac{\left\|h_{21}^{k_1}\right\|^2}{\left\|h_{22}^{k_2}\right\|^2} \geq \frac{N_1}{N_2}, \frac{N_2}{N_1} + \frac{P_2\left\|h_{22}^{k_2}\right\|^2}{N_1} \geq \frac{\left\|h_{12}^{k_2}\right\|^2}{\left\|h_{11}^{k_1}\right\|^2} \geq \frac{N_2}{N_1}, \frac{P_1\left(\left\|h_{11}^{k_1}\right\|^2 N_2 - \left\|h_{12}^{k_2}\right\|^2 N_1\right)}{P_2\left(\left\|h_{22}^{k_2}\right\|^2 N_1 - \left\|h_{21}^{k_1}\right\|^2 N_2\right)} < 1$	C_2	$(0,0)$
Strongly mixed I	$\frac{\left\|h_{21}^{k_1}\right\|^2}{\left\|h_{22}^{k_2}\right\|^2} > \frac{N_1 + P_1\left\|h_{11}^{k_1}\right\|^2}{N_2 + P_1\left\|h_{12}^{k_2}\right\|^2}, \frac{N_2}{N_1} > \frac{\left\|h_{12}^{k_2}\right\|^2}{\left\|h_{11}^{k_1}\right\|^2} \geq 0$	C_3	$(1,0)$
Strongly mixed II	$\frac{N_1}{N_2} > \frac{\left\|h_{21}^{k_1}\right\|^2}{\left\|h_{22}^{k_2}\right\|^2} \geq 0, \frac{\left\|h_{12}^{k_2}\right\|^2}{\left\|h_{11}^{k_1}\right\|^2} > \frac{N_2 + P_2\left\|h_{22}^{k_2}\right\|^2}{N_1 + P_2\left\|h_{21}^{k_1}\right\|^2}$	C_4	$(0,1)$
Weakly mixed I	$\frac{N_1 + P_1\left\|h_{11}^{k_1}\right\|^2}{N_2 + P_1\left\|h_{12}^{k_2}\right\|^2} \geq \frac{\left\|h_{21}^{k_1}\right\|^2}{\left\|h_{22}^{k_2}\right\|^2} \geq \frac{N_1}{N_2}, \frac{N_2}{N_1} > \frac{\left\|h_{12}^{k_2}\right\|^2}{\left\|h_{11}^{k_1}\right\|^2} \geq 0$	C_2	$(1,0)$
Weakly mixed II	$\frac{N_1}{N_2} > \frac{\left\|h_{21}^{k_1}\right\|^2}{\left\|h_{22}^{k_2}\right\|^2} \geq 0, \frac{N_2 + P_2\left\|h_{22}^{k_2}\right\|^2}{N_1 + P_2\left\|h_{21}^{k_1}\right\|^2} \geq \frac{\left\|h_{12}^{k_2}\right\|^2}{\left\|h_{11}^{k_1}\right\|^2} \geq \frac{N_2}{N_1}$	C_1	$(0,1)$
Somewhat weak I	$\frac{N_1}{N_2} > \frac{\left\|h_{21}^{k_1}\right\|^2}{\left\|h_{22}^{k_2}\right\|^2} > \frac{N_1}{N_2 + P_1\left\|h_{12}^{k_2}\right\|^2}, \frac{N_2}{N_1 + P_2\left\|h_{21}^{k_1}\right\|^2} \geq \frac{\left\|h_{12}^{k_2}\right\|^2}{\left\|h_{11}^{k_1}\right\|^2}$	C_2	$(1,0)$
Somewhat weak II	$\frac{N_1}{N_2 + P_1\left\|h_{12}^{k_2}\right\|^2} \geq \frac{\left\|h_{21}^{k_1}\right\|^2}{\left\|h_{22}^{k_2}\right\|^2}, \frac{N_2}{N_1} > \frac{\left\|h_{12}^{k_2}\right\|^2}{\left\|h_{11}^{k_1}\right\|^2} > \frac{N_2}{N_1 + P_2\left\|h_{21}^{k_1}\right\|^2}$	C_1	$(0,1)$
Barely weak I	$\frac{N_1}{N_2} > \frac{\left\|h_{21}^{k_1}\right\|^2}{\left\|h_{22}^{k_2}\right\|^2} > \frac{N_1}{N_2 + P_1\left\|h_{12}^{k_2}\right\|^2}, \frac{N_2}{N_1} > \frac{\left\|h_{12}^{k_2}\right\|^2}{\left\|h_{11}^{k_1}\right\|^2} > \frac{N_2}{N_1 + P_2\left\|h_{21}^{k_1}\right\|^2}$, $P_1\left(\left\|h_{11}^{k_1}\right\|^2 N_2 - \left\|h_{12}^{k_2}\right\|^2 N_1\right) \geq P_2\left(\left\|h_{22}^{k_2}\right\|^2 N_1 - \left\|h_{21}^{k_1}\right\|^2 N_2\right),\ f(\tilde{\lambda}_1, \tilde{\lambda}_2) \leq 1,\ f(\hat{\lambda}_1, \hat{\lambda}_2) \leq 1$	C_2	$(1,0)$
Barely weak II	$\frac{N_1}{N_2} > \frac{\left\|h_{21}^{k_1}\right\|^2}{\left\|h_{22}^{k_2}\right\|^2} > \frac{N_1}{N_2 + P_1\left\|h_{12}^{k_2}\right\|^2}, \frac{N_2}{N_1} > \frac{\left\|h_{12}^{k_2}\right\|^2}{\left\|h_{11}^{k_1}\right\|^2} > \frac{N_2}{N_1 + P_2\left\|h_{21}^{k_1}\right\|^2}$, $P_1\left(\left\|h_{11}^{k_1}\right\|^2 N_2 - \left\|h_{12}^{k_2}\right\|^2 N_1\right) < P_2\left(\left\|h_{22}^{k_2}\right\|^2 N_1 - \left\|h_{21}^{k_1}\right\|^2 N_2\right),\ c > f(\tilde{\lambda}_1, \tilde{\lambda}_2),\ c > f(\hat{\lambda}_1, \hat{\lambda}_2)$	C_1	$(0,1)$
Barely weak III	$\frac{N_1}{N_2} > \frac{\left\|h_{21}^{k_1}\right\|^2}{\left\|h_{22}^{k_2}\right\|^2} > \frac{N_1}{N_2 + P_1\left\|h_{12}^{k_2}\right\|^2}, \frac{N_2}{N_1} > \frac{\left\|h_{12}^{k_2}\right\|^2}{\left\|h_{11}^{k_1}\right\|^2} > \frac{N_2}{N_1 + P_2\left\|h_{21}^{k_1}\right\|^2}, \tilde{\lambda}_2 < \hat{\lambda}_2$ or $f(\hat{\lambda}_1, \hat{\lambda}_2) < f(\tilde{\lambda}_1, \tilde{\lambda}_2)$	C_5	$(\tilde{\lambda}_1, \tilde{\lambda}_2)$
Barely weak IV	$\frac{N_1}{N_2} > \frac{\left\|h_{21}^{k_1}\right\|^2}{\left\|h_{22}^{k_2}\right\|^2} > \frac{N_1}{N_2 + P_1\left\|h_{12}^{k_2}\right\|^2}, \frac{N_2}{N_1} > \frac{\left\|h_{12}^{k_2}\right\|^2}{\left\|h_{11}^{k_1}\right\|^2} > \frac{N_2}{N_1 + P_2\left\|h_{21}^{k_1}\right\|^2}, \tilde{\lambda}_2 \geq \hat{\lambda}_2,\ f(\hat{\lambda}_1, \hat{\lambda}_2) \geq f(\tilde{\lambda}_1, \tilde{\lambda}_2),$	C_6	$(\hat{\lambda}_1, \hat{\lambda}_2)$
Very weak	$\frac{N_1}{N_2 + P_1\left\|h_{12}^{k_2}\right\|^2} \geq \frac{\left\|h_{21}^{k_1}\right\|^2}{\left\|h_{22}^{k_2}\right\|^2}, \frac{N_2}{N_1 + P_2\left\|h_{21}^{k_1}\right\|^2} \geq \frac{\left\|h_{12}^{k_2}\right\|^2}{\left\|h_{11}^{k_1}\right\|^2}$	C_7	$(1,1)$

and

$$n = \frac{P_1\left(\left\|h_{11}^{k_1}\right\|^2 N_2 - \left\|h_{12}^{k_2}\right\|^2 N_1\right) - P_2\left(\left\|h_{22}^{k_2}\right\|^2 N_1 - \left\|h_{21}^{k_1}\right\|^2 N_2\right)}{P_1\left(\left\|h_{11}^{k_1}\right\|^2 N_2 - \left\|h_{12}^{k_2}\right\|^2 N_1 + P_2\left(\left\|h_{22}^{k_2}\right\|^2 \left\|h_{11}^{k_1}\right\|^2 - \left\|h_{21}^{k_1}\right\|^2 \left\|h_{12}^{k_2}\right\|^2\right)\right)}.$$

In addition,

$$\tilde{\lambda}_1 = \frac{\left\|h_{21}^{k_1}\right\|^2\left(P_1\left\|h_{12}^{k_2}\right\|^2 + N_2\right) - \left\|h_{22}^{k_2}\right\|^2 N_1}{P_1\left\|h_{11}^{k_1}\right\|^2\left\|h_{22}^{k_2}\right\|^2},$$

$$\tilde{\lambda}_2 = \frac{\left\|h_{12}^{k_2}\right\|^2\left(P_2\left\|h_{21}^{k_1}\right\|^2 + N_1\right) - \left\|h_{11}^{k_1}\right\|^2 N_2}{P_2\left\|h_{11}^{k_1}\right\|^2\left\|h_{22}^{k_2}\right\|^2}.$$

Given the closed-form solutions to (10), (8) is now reduced to

$$\max_{\boldsymbol{k} \in \mathcal{K}} R^*_{\mathrm{HKF}}(\boldsymbol{k}). \tag{11}$$

This problem can be solved by searching the optimal ports over $M_1 M_2$ possible combinations. Note that the global optimality of the solutions is guaranteed by hierarchical structure. Since the ports in FAS provide additional opportunity to improve the maximum sum-rate, the performance of HK-FAMA is at least as good as that of the HK scheme.

IV. PERFORMANCE EVALUATION

In this section, we discuss FAMA and other benchmarking schemes. In addition, we introduce a new performance metric that is useful for explaining the principle of FAMA.

A. FAMA and Other Benchmarking Schemes

Compared to HK-FAMA and HK, FAMA is a much simpler scheme since no power splitting, rate splitting and joint decoding/successive interference cancellation are required. More

precisely, FAMA treats interference as noise and is a special case of HK-FAMA with $(\gamma_1, \gamma_2) = (1, 1)$. Nevertheless, the optimal port of FAMA might be different from that of HK-FAMA. In FAMA, each receiver r selects the port with the highest signal-to-interference plus noise ratio (SINR) [6], i.e.,

$$k_r^\star = \underset{k_r \in \{1,\ldots,M_r\}}{\arg\max} \left\{ \frac{\left|h_{rr}^{k_r}\right|^2 P_r}{\left|h_{r'r}^{k_r}\right|^2 P_{r'} + N_r} \right\}, \tag{12}$$

and thus the maximum sum-rate is

$$R_{\mathrm{F}}^* = \log\left(1 + \frac{\left|h_{11}^{k_1^\star}\right|^2 P_1}{\left|h_{21}^{k_1^\star}\right|^2 P_2 + N_1}\right) + \log\left(1 + \frac{\left|h_{22}^{k_2^\star}\right|^2 P_2}{\left|h_{12}^{k_2^\star}\right|^2 P_1 + N_2}\right). \tag{13}$$

If $k_r, \forall r$ is fixed, FAMA is then equivalent to the traditional treating interference as noise (TIN) scheme.

In addition, we consider the traditional orthogonalization (ORTHO) scheme where $k_r, \forall r$ is fixed and half of the degree of freedom is given to each receiver. The maximum sum-rate of ORTHO is given by

$$R_{\mathrm{O}}^* = \tfrac{1}{2}\log\left(1 + \frac{\left|h_{11}^{k_1}\right|^2 P_1}{\frac{N_1}{2}}\right) + \tfrac{1}{2}\log\left(1 + \frac{\left|h_{22}^{k_2}\right|^2 P_2}{\frac{N_2}{2}}\right). \tag{14}$$

B. Generalized Degree of Freedom

To reveal the principle of FAMA, we extend the concept of generalized degree of freedom (gdof) in symmetric channel [9] to non-symmetric reconfigurable channel for FAS with finite signal-to-noise ratio (SNR).[3] Specifically, the gdof of a scheme is defined as

$$\mathrm{gdof} \triangleq \frac{R_{\mathrm{sys}}(\boldsymbol{k})}{C^*}, \tag{15}$$

where $R_{\mathrm{sys}}(\boldsymbol{k})$ is the maximum sum-rate of a scheme and $C^* = \max\limits_{\boldsymbol{k}\in\mathcal{K}} \log\left(1 + \frac{P_1\left|h_{11}^{k_1}\right|^2}{N_1}\right) + \log\left(1 + \frac{P_2\left|h_{22}^{k_2}\right|^2}{N_2}\right)$. The gdof can be interpreted as the ratio of the maximum sum-rate of a scheme to the maximum possible sum-rate without interference. Therefore, if $R_{\mathrm{sys}}(\boldsymbol{k}) = C^*$, we can say that the interference has no effect on the receivers and thus the overall links have full degree of freedom. In contrast, if $R_{\mathrm{sys}}(\boldsymbol{k}) = 0$, the interference has significant effect on the receivers such that no communication is possible and thus the overall links have zero degree of freedom. Furthermore, let us define

$$\alpha \triangleq \frac{\log(a\,\mathrm{SNR}_2)}{\log(\mathrm{SNR}_1)}, \tag{16}$$

and

$$\beta \triangleq \frac{\log(b\,\mathrm{SNR}_1)}{\log(\mathrm{SNR}_2)}, \tag{17}$$

where $a = \frac{\left|h_{21}^{k_r}\right|^2 N_2}{\left|h_{22}^{k_r}\right|^2 N_1}$, $b = \frac{\left|h_{12}^{k_r}\right|^2 N_1}{\left|h_{11}^{k_r}\right|^2 N_2}$, $\mathrm{SNR}_1 = \frac{P_1\left|h_{11}^{k_r}\right|^2}{N_1}$ and $\mathrm{SNR}_2 = \frac{P_2\left|h_{22}^{k_r}\right|^2}{N_2}$. Heuristically, we can interpret α and β as the ratio of interference-to-noise ratio to SNR, in decibels. If $\alpha = \beta$, we have symmetric channel. If α or $\beta \geq 0$, the system is operating in the interference-limited regime. Otherwise, it is operating in the noise-limited regime.

[3]A finite SNR is considered here because reconfigurable channel is only useful when SNR is not asymptotically high.

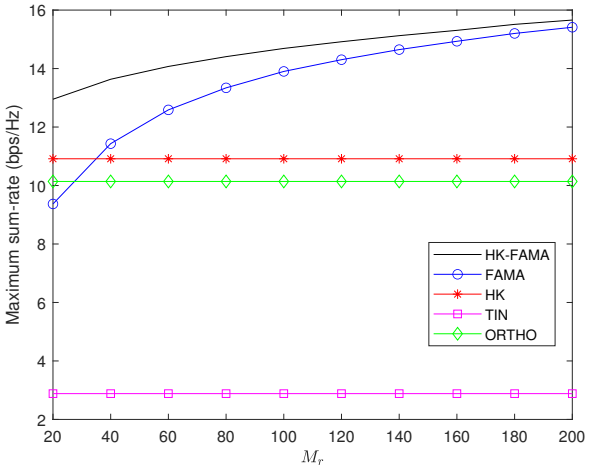

Figure 2. The maximum sum-rate over different values of M_r.

V. Simulation Results

In this section, we present the simulation results to evaluate the performance of different schemes as well as to reveal the underlying principle of FAMA. For brevity, we consider the setting where $P_1 = P_2 = P$, $N_1 = N_2 = N_0$, $M_1 = M_2$, $M_1^r = 2M_2^r$, $W_1 = W_2$ and $W_1^r = 2W_2^r$. Unless stated otherwise, we set $P = 30$ dBm, $N_0 = 0$ dBm, $\sigma_{t,r} = 1$, $M_r = M_1^r \times M_2^r = 20 \times 10$, $W_r = W_1^r \times W_2^r = 2\lambda \times 1\lambda$. In the HK, TIN and ORTHO schemes, we assume that $k_r = 1$.

Firstly, we compare the maximum sum-rate over different values of M_r where we fix $M_2^r = 10$. As confirmed in Fig. 2, HK-FAMA has the highest sum-rate because it can select the best channel and employ the best strategy in each reconfigured channel. Interestingly, the sum-rate of FAMA approaches to that of HK-FAMA as M_r increases. This suggests that treating interference as noise is near-optimal if there is a sufficient number of ports. Nevertheless, when M_r is small, the channel cannot be greatly reconfigured. Therefore, the sum-rates of HK and ORTHO can be higher than that of FAMA as treating interference as noise is a suboptimal strategy. Furthermore, TIN has the worst performance because the channel cannot be reconfigured and its strategy is far from optimal.

Next in Fig. 3, we compare the maximum sum-rate over different values of W_r. Here, we fix $W_2^r = 1\lambda$. Similarly, HK-FAMA has the highest sum-rate and the sum-rate of FAMA again approaches to that of HK-FAMA as W_r increases. In contrast to the above, the performance of FAMA outperforms HK, TIN and ORTHO since M_r is sufficiently large here. If we increase M_r from 20×10 to 30×10, the sum-rates of HK-FAMA and FAMA shift upward and their gap reduces.

Fig. 4 shows the distributions of α and β over 300 independent realizations to explain the principle of FAMA. Here, we plot the maximum gdof that can be achieved by any schemes as a contour.[4] This contour can be used as a reference to under-

[4]This can be done using HK with a deterministic channel. Specifically, we assume that $|h_{1,1}|^2 = |h_{2,2}|^2 = 1$ and vary α and β accordingly.

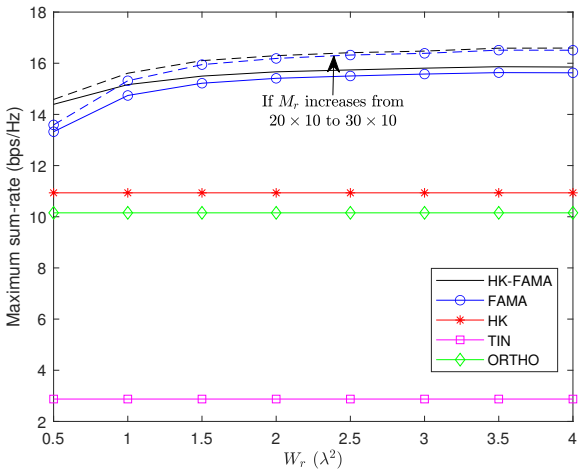

Figure 3. The maximum sum-rate over different values of W_r.

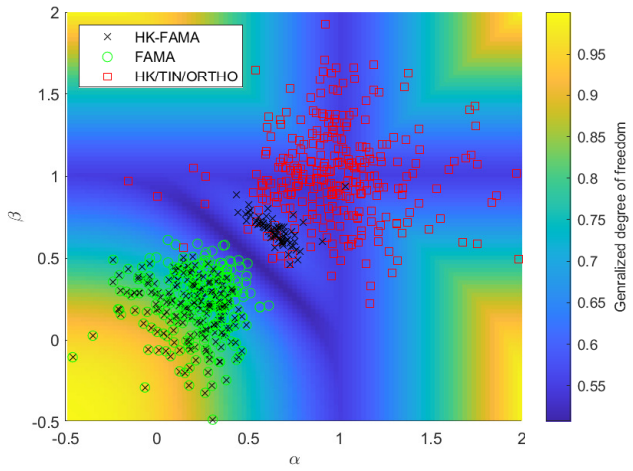

Figure 4. Distributions of of α and β for different schemes.

stand the relation between the distributions and performance of the schemes. Note that HK, TIN and ORTHO have the same α and β since k_r is fixed. Nevertheless, they have different gdof. Thus, it is important to study their average gdof. The average gdof of HK-FAMA, FAMA, HK, TIN and ORTHO are 0.65, 0.64, 0.46, 0.13 and 0.43, respectively.

In Fig. 4, we can observe that TAS is unable to reconfigure the channel. Therefore, the distributions of HK/TIN/ORTHO depend entirely on the given realizations. Based on their average gdof, we deduce that it is important for TAS to use HK to obtain higher gdof but ORTHO is pretty sufficient. In contrast, HK-FAMA and FAMA have the ability to reconfigure the channel (e.g., they can adjust the values of α and β). In principle, if M_r and W_r are sufficiently large, both of these schemes tend to make the values of α and β small to obtain a higher gdof. Nevertheless, in some realizations, HK-FAMA might choose larger α and β to avoid low gdof (e.g., dark blue zone). Those are the moments where FAMA is not efficient. Otherwise, treating interference as noise in FAMA is optimal. If M_r and W_r are increased, it is easier for their distributions to overlap and operate towards the noise-limited regime.

VI. Conclusion

This paper considered two transmitter-receiver pairs where each receiver was equipped with a 2D surface fluid antenna. To study whether treating interference as noise in FAMA is an efficient strategy in this setting, we introduced a new benchmarking scheme, namely HK-FAMA. We maximized the sum-rate of HK-FAMA via joint optimal port selection, power splitting and rate splitting. Compared to HK-FAMA and other benchmarking schemes, we showed that FAMA can be near to being optimal as the channel can be reconfigured towards the noise-limited regime where high gdof can be obtained. Thus, complicated schemes are not always necessary as treating interference as noise in FAMA is sufficient. Nevertheless, to facilitate such channel reconfiguration, M_r and W_r must be sufficiently large.

Acknowledgment

This work is supported by the Engineering and Physical Sciences Research Council (EPSRC) under grant EP/W026813/1.

References

[1] K. K. Wong, K. F. Tong, Y. Shen, Y. Chen, and Y. Zhang, "Bruce Lee-inspired fluid antenna system: Six research topics and the potentials for 6G," *Frontiers Commun. and Netw.*, p. 5, 2022.

[2] L. Tlebaldiyeva, S. Arzykulov, K. M. Rabie, X. Li, G. Nauryzbayev, "Outage performance of fluid antenna system (FAS)-aided Terahertz communication networks", in Proc. *IEEE Inter. Conf. Commun. (ICC)*, 28 May-1 Jun. 2023, Rome, Italy.

[3] C. Skouroumounis and I. Krikidis, "Fluid antenna with linear MMSE channel estimation for large-scale cellular networks," in *IEEE Trans. Commun.*, vol. 71, no. 2, pp. 1112-1125, Feb. 2023.

[4] M. Khammassi, A. Kammoun and M. S. Alouini, "A new analytical approximation of the fluid antenna system channel," in *IEEE Trans. Wireless Commun.*, 2023 (early access).

[5] W. K. New, K. K. Wong, H. Xu, K. F. Tong and C. B. Chae, "An information-theoretic characterization of MIMO-FAS: Optimization, diversity-multiplexing tradeoff and q-outage capacity," [Online] arXiv:2303.02269, 2023.

[6] K. K. Wong, D. Morales-Jimenez, K. F. Tong and C. B. Chae, "Slow fluid antenna multiple access," in *IEEE Trans. Commun.*, vol. 71, no. 5, pp. 2831-2846, May 2023, doi: 10.1109/TCOMM.2023.3255904.

[7] H. Xu, K. K. Wong, W. K. New, and K. F. Tong, "On the outage probability for two-user fluid antenna multiple access," in Proc. *IEEE Inter. Conf. Commun. (ICC)*, 28 May-1 Jun. 2023, Rome, Italy.

[8] B. Clerckx *et al.*, "A primer on rate-splitting multiple access: Tutorial, myths, and frequently asked questions," in *IEEE J. Select. Areas Commun.*, vol. 41, no. 5, pp. 1265-1308, May 2023, doi: 10.1109/JSAC.2023.3242718.

[9] R. H. Etkin, D. N. C. Tse, and H. Wang, "Gaussian interference channel capacity to within one bit," *IEEE Trans. Info. Theory*, vol. 54, no. 12, pp. 5534–5562, Dec. 2008.

[10] A. Haghi and A. K. Khandani, "Boundary of the Gaussian Han-Kobayashi rate region," *IEEE Trans. Info. Theory*, vol. 67, no. 4, pp. 2034–2054, Apr. 2021.

[11] H. Sato, "The capacity of the Gaussian interference channel under strong interference," *IEEE Trans. Info. Theory*, vol. 27, no. 6, pp. 786–788, Nov. 1981.

[12] A. S. Motahari and A. K. Khandani, "Capacity bounds for the Gaussian interference channel," *IEEE Trans. Info. Theory*, vol. 55, no. 2, pp. 620–643, Feb. 2009.

[13] H.-F. Chong, M. Motani, H. K. Garg, and H. El Gamal, "On the Han-Kobayashi region for the interference channel," *IEEE Trans. Info. Theory*, vol. 54, no. 7, pp. 3188–3195, Jul. 2008.